

Received 30 September 2023, accepted 2 November 2023, date of publication 6 November 2023, date of current version 14 November 2023.

Digital Object Identifier 10.1109/ACCESS.2023.3330587

## RESEARCH ARTICLE

# Establishment of Real-Time Adaptive Control Strategy for Milling Parameters

CHIH-HO TAI<sup>ID</sup>, YING-TE TSAI, AND KUAN-MING LI<sup>ID</sup>

Department of Mechanical Engineering, National Taiwan University, Taipei 10671, Taiwan

Corresponding author: Kuan-Ming Li (kml@ntu.edu.tw)

This work was supported in part by the National Science and Technology Council, Taiwan, under Grant NSTC 112-2218-E-002-045 and Grant NSTC 111-2221-E-002-142.

**ABSTRACT** The traditional method of milling which uses constant spindle speed and feedrate to prevent machine, workpiece, and machining tool failure. However, this method prevents engineers from further improving machining efficiency. It is possible to increase machining efficiency by appropriately adjusting feedrate during the machining process. Although there are plenty of researches regarding adaptive machining force control, those researches focus on the design of controller, and few of them discuss the relation between control signals and tool wear for parameters setting. This study presents a method for setting process parameters in constant load machining, including feedrate upper and lower limits, as well as reference spindle current. The reference spindle current and feedrate upper limit were selected to sustain cutting force up to tool strength. The feedrate lower limit was established to maintain tool wear conditions within a given range, preventing severe and unstable tool wear. The experimental results showed that when the feedrate was reduced to the lower limit value, the machining parameters setting method presented in this study could keep the tool wear within the set value, avoiding the risk of tool failure. The strategy for setting the machining parameters can be used to end milling, slot milling, or a combination of both milling processes. The constant load machining parameters presented in this study outperformed constant feedrate machining of the identical milling conditions in terms of tool life and material removal rate. The traditional method estimated tool life by cutting lengths, but we used the feedrate change to estimate the tool wear for change. The result showed that this method had better tool life than traditional way.

**INDEX TERMS** Adaptive machining, constant load machining, force control, spindle current, tool wear.

## I. INTRODUCTION

In recent years, CNC (Computer Numeric Control) machining has been widely used in different industries to manufacture molds and critical parts. In the development stage of industrial products, CNC machining can quickly manufacture high-precision metal parts. Therefore, it is often used to produce aerospace engineering parts. Due to the wide range of applications and the demand for mass production, the monitoring technology of the machining process is thriving to improve processing efficiency [1], [2], [3], [4]. The Internet of Things is driving Industry 4.0 development [5], [6], [7], and CNC machining is likewise evolving toward a more advanced

network of machines and systems. Industry 4.0 has significantly increased processing performance; yet, the strategy for defining CNC machining parameters remains one of the most fundamental and critical concerns in machining.

Traditionally, constant spindle speed and feedrate have been widely adopted in milling, most of which are conservative machining conditions, to prevent machine, workpiece, and cutting tool failure. This method ensures the stability and reliability of the milling process, but on the other hand, prevents engineers to further improving machining efficiency. Through an adaptive machining force control system, it's possible to increase machining efficiency by appropriately adjusting feedrate during the machining process. Koren et al. [8] proposed the concept of ACC (Adaptive Control with Constraints) to control the processing system

The associate editor coordinating the review of this manuscript and approving it for publication was Chao-Yang Chen<sup>ID</sup>.

by using the cutting force. After the sensor captured the data through signal analysis and visualization processing, a controller was designed to control the processing parameters and increase processing efficiency, quality, and stability. Lauderbaugh et al. [9] established a dynamic model for responding to feedrate changes and processing forces in the manufacturing process using the ACC system and control theory tools. Fixed processing parameters may cause poor processing results when cutting conditions change significantly. They used the dynamic model to alleviate the problem. Koren and Ulsoy's studies [10], [11] have shown that using the adaptive control theory to control the cutting force can improve efficiency and workpiece quality. Liu et al. proposed to design feedback control and various controllers in ACC machining to establish an ACC machining control system [12], [13]. They compared the advantages and disadvantages of different ACC systems. Yang et al. [14], [15] investigated several control algorithms to establish an ACC system that adjusts the spindle current for milling. It has been demonstrated that altering the spindle current may control the output of the machining force in a stable manner and has broad applicability.

When the cutting tool gradually wears away, deterioration of surface roughness is observed. Tool wear is an important factor that influences surface roughness and dimensional accuracy. Mohamed et al. proposed that the integration of a tool condition monitoring system with ACC system could enable optimization of tool remaining life [16]. Huang et al. [17] used convolutional neural networks for a multi-domain analysis extracted from cutting forces and vibration in the dry milling process to create a multi-domain model for tool wear prediction. Gorka et al. [18] proposed a monitoring system for the simultaneous recording of machining forces, accelerations, noise and acoustic pressure. Lacalle et al. [19], [20] proposed a system for diagnosing the milling process by simultaneously collecting cutting forces and cutting tool positions (coordinates X, Y, and Z). Mohanraj et al. [21] developed the tool condition monitoring system in the end milling process using wavelet features and Hoelder's exponent with machine learning algorithms. Laboratories worldwide have developed many tool condition monitoring systems to detect tool wear, chipping, and breakage. Various Neuro-Fuzzy technologies for data collection and processing have been proposed in an attempt to develop surface quality prediction models [22], [23]. However, these research methods are not simple and cannot be easily applied to the actual milling production line. Yuan et al. [24] used the spindle current signal and the features of the machined surface image to find a connection between the tool wear condition and the process signals. Studies also used the fractal analysis of the spindle current signals as a method for tool condition monitoring [25], [26]. Monitoring the tool wear using the spindle current signal is relatively simple. Lee et al. [27] suggested using the decrease in feedrate as a basis for evaluating tool wear when controlling the spindle load. This method is more

easily applied in actual machining. When the tool gradually wears out in ACC machining and produces a poor surface roughness, it is a practical method to lower the feedrate to maintain the surface roughness and the same cutting force during the cutting process. Kim et al. [28] successfully developed a control system to sense cutting forces by measuring spindle motor current, rather than using an expensive and impractical tool dynamometer. However, the method and strategy for setting the ACC system's parameters still have to be examined.

Thlusty [29] analyzed the transient response of an adaptive control servomechanism for constant force milling. Its robustness was affected by system noise or unmodeled dynamics. Its adaptability and robustness did not maintain a good state in the case of simultaneous changes in the environment and system drift. The fuzzy set theory has been successfully applied to control problems [30], [31]. This method has good robustness and model-free properties. However, fuzzy controllers require expert knowledge or operator experience to establish appropriate control rules and membership functions. Saldago et al. [32] used current and acoustic signals for in-process tool wear monitoring. Zuperl et al. [33] designed a neural constant force controller using adaptive regulation of the feedrate to prevent excessive tool wear, and tool breakage and maintain a high chip removal rate. But those researches focus on the design of controllers and their computational algorithm, and few discuss the relation between control signals and tool wear for parameters setting. This research will establish the relationship between feedrate, spindle current, and tool wear. The relation can be a reference when setting machining parameters and wear monitoring in adaptive machining force control. To study the method of setting the ACC system's parameters, this research uses spindle current instead of cutting force as input signals to establish constant load milling. The relationship between feedrate with tool wear and spindle load current is investigated through constant feedrate experiments. According to experimental results, a reasonable strategy for setting process parameters is proposed. The selected processing parameters are applied to slot milling, end milling, and a combination of slot milling and end milling to verify the applicability of the proposed method. Constant load machining is to improve machining efficiency by adjusting the feedrate according to the spindle current so the surface finish could not achieve high quality. Because tool wear was considered when setting the parameters for constant load machining, the application of this study targets at semi-precision machining. The change of feedrate in constant load milling was used as an auxiliary index to determine the timing of tool change to reduce the downtime to inspect cutting tools. The proposed method is also evaluated by examining the impact on tool life and material removal rate. Surface roughness was measured in each cutting test. Nevertheless, there was not any trend of surface roughness regarding to the cutting parameters in this study. The process quality was not emphasized.

II. CONSTANT LOAD MACHINING

A. THEORETICAL BACKGROUND

The dynamic equation of the machine tool spindle can be expressed by the following equation:

$$K_t I_M = J \frac{d\omega}{dt} + B_M \omega + T_f + T_d \tag{1}$$

$K_t$  is the spindle motor-torque constant,  $I_M$  is the spindle current,  $J$  is the moment of inertia of the motor,  $\omega$  is the spindle speed,  $B_M$  is the damping coefficient,  $T_f$  is the Coulomb friction torque, and  $T_d$  is the torque produced by the machining forces on the spindle in machining [15], [34].

The machining experiment in this study used a fixed spindle speed for processing so that the following equation can be obtained:

$$\frac{d\omega}{dt} = 0 \tag{2}$$

The disturbance torque was assumed to be related to the mean cutting force  $F_c$  as follows:

$$T_d = r F_c \tag{3}$$

where  $r$  is the tool radius.

Because damping torque and Coulomb friction torque are dependent on the machine tools, they can be assumed to be constant for a fixed machine tool as follows:

$$B_M \omega + T_f = C_s \tag{4}$$

Substituting (2)-(4) into (1), (1) can be simplified as (5) [35]:

$$K_t I_M = C_s + r \cdot F_c \tag{5}$$

To determine the relationship between cutting force and feedrate in an end mill, the cutting tool was divided into disc elements of thin thickness. In a single disc element, when the rotational speed of the cutting is sufficiently fast compared to its feedrate, the motion of the cutting edge can be approximated as a circular trajectory [36].

The chip thickness  $t_c$  is approximated by:

$$t_c = f_t \sin \alpha \tag{6}$$

where  $f_t$  is the feed per tooth (mm/tooth), and is the tool engagement angular position of a tooth. The instantaneous resultant cutting force is represented as follows:

$$F = \sum_{k=1}^{N_t} \int_0^{d_a} K_f f_t \sin \alpha dz \tag{7}$$

where  $N_t$  is the number of flutes of the end mill,  $d_a$  is the axial depth of cut, and  $K_f$  is the specific cutting coefficient of the work material.

Since the axial position on the cutter from its end  $z$  is related to the angular position and the cutter radius  $r$  by (8), the instantaneous cutting force can be expressed as (9) by replacing the integral parameter  $z$  with the angular position  $\alpha$  from (7).

$$\alpha = \frac{\tan \alpha_h}{r} z \tag{8}$$

$$F_i = \sum_{k=1}^{N_t} \int_0^{d_a} K_f \frac{r}{\tan \alpha_h} f_t \sin \alpha d\alpha \tag{9}$$

where  $\alpha_h$  is the helix angle of the end mill [36].

Through the integration of the instantaneous cutting force during one revolution of the tool, the mean cutting force  $F_c$  can be obtained:

$$F_c = \frac{\int_0^{2\pi} \left( \sum_{k=1}^{N_t} \int_0^{d_a} K_f \frac{r}{\tan \alpha_h} f_t \sin \alpha d\alpha \right) d\phi}{2\pi/N_t} f_t \tag{10}$$

where  $\phi$  is the tool rotation angle [36]. Since feed is unrelated to the integral parameters, it is taken out of the integral as in (10).

Consequently, the relationship between spindle current and feedrate can be obtained by substituting (10) into (5):

$$K_t I_M = C_s + r \frac{\int_0^{2\pi} \left( \sum_{k=1}^{N_t} \int_0^{d_a} K_f \frac{r}{\tan \alpha_h} f_t \sin \alpha d\alpha \right) d\phi}{2\pi/N_t} f_t \tag{11}$$

Since the machine tool, cutting tool and workpiece material in the experiments are fixed, (11) can be simplified to (12) [14]:

$$I_M = A + B \cdot f_t \tag{12}$$

where parameter  $A$  is determined by the CNC machine and parameter  $B$  is related to the cutting tool, workpiece, CNC machine and cutting conditions. When the cutting tool, workpiece, machine tool and cutting condition are fixed, a simple linear relationship exists between the spindle current and the feed per tooth, and the slope is  $B$ . Since the feedrate is a common parameter used in machine tools, (12) is rewritten as follows:

$$I_M = A + B \cdot f_m \tag{13}$$

where  $f_m$  is the feedrate, parameter  $A$  is the idle spindle current when the feedrate is zero, and  $B$  is the coefficient determined by cutting tests [15]. Equation (13) shows a linear relationship between the spindle current and feedrate, considering a new tool without wear. When tool wear begins, the machining force will increase accordingly. Therefore, when the tool wears, the feedrate must decrease if the constant cutting load is desired. As a result, the spindle reference current, the upper limit of the feedrate, and the lower limit of the feedrate for constant load milling have to be determined before (13) is applied to the machining processes.

When considering the additional force due to tool wear by (13), the relationship among tool wear and cutting force is assumed to be represented as (14) [27]:

$$I_M = A + B \times f_m + k_1 \times V_B \tag{14}$$

where  $V_B$  is the flank wear width,  $k_1$  is the flank wear coefficient.

According to the purpose of constant load machining when considering tool wear, the feedrate decreases with respect to

tool wear can be represented as (15):

$$f_m = \frac{I_M - A}{B} - \frac{k_1}{B} \times V_B \quad (15)$$

The constant load control was applied by real-time feedrate override to the CNC controller. To reduce the effect of signal fluctuations on feedrate override, the moving average of the feedrate override was employed.

According to (15),  $f_m$  is the maximum and upper limit of feedrate when  $V_B$  is zero. As the tool wear increases, the feedrate should gradually decrease, where  $V_B$  and feedrate have a linear relationship. And the flank wear can be used to determine the lower limit of the feedrate [15]. As a result, after calculating the reference current for constant load machining and the maximum flank wear when the tool needs to be changed, constant feedrate wear experiments can be used to set the lower limit of feedrate. According to (15),  $f_m$  is the minimum and lower limit of feedrate when  $V_B$  reaches the maximum.

### B. CONTROLLER DESIGN FOR CONSTANT LOAD MILLING

Setting the reference spindle current and feedrate upper and lower limits are the objectives of this study. A PI (proportional–integral) controller [37], [38] was used for control. The controller used in this study was governed by the following equation:

$$U = U_0 + K_p \times e(t) + K_i \times \int_0^t e(t) dt \quad (16)$$

where  $U$  represents the signal under control,  $U_0$  is the last control signal,  $e(t)$  is the current error value (set value minus measured value). Other parameters included the proportional gain ( $K_p$ ), and the integral gain ( $K_i$ ).

The spindle load generated during the machining process was feedback to the controller through the current hook meter (FLUKE i-200s). After the controller compared the reference value with this signal, it output a new feed command to stabilize the spindle load.

### C. RESEARCH PROCESS

The research flow of setting process parameters for constant load machining is shown in Figure 1. First, find the relationship between feedrate, spindle load current, and flank wear of slot milling and end milling with constant feedrate experiments. In this study, the spindle reference current and the upper limit of feedrate were set based on the maximum cutting force that the tool could bear to achieve the highest material removal rate. The end of tool flank wear interval was used for setting the lower limit of the feedrate, and the feedrate as a real-time signal reference for tool change. Second, carry out constant load machining, including slot milling and end milling experiments, to verify the correctness and repeatability of the strategy for setting machining parameters.

Third, verify the proposed strategy of process parameter setting by applying mixed machining tool paths of slot milling and end milling. Perform machining with constant load milling, and verify tool change timing.

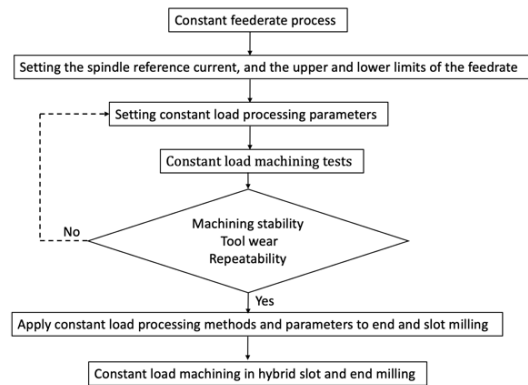


FIGURE 1. Research flow for constant load machining.

### D. THE CONTROL SYSTEM OF CONSTANT LOAD MILLING

Previous studies [14], [15] have pointed out that the machining force is closely related to the spindle current. The machine tool is a five-axis machine developed by the Precision Machinery Research Center (PMC). The constant load milling controller is designed using the LabVIEW software [39] environment. The architecture of the closed-loop control system and hardware equipment used in this study are shown in Figures 2(a) and 2(b). The experimental set up is shown in Figure 2(c). The data acquisition card used was NI USB-6431. The control system mainly comprised the current hook meter, the LabVIEW PID controller, and the data acquisition card (NI USB-6431) to output control signals. The spindle load current was measured by the current hook meter (Fluke i-200s) and recorded by the computer. The data acquisition card output the control signal as Zero-order Hold voltage. The ADC conversion card converted the analog signal to a digital signal (SYNTEC TB16IN-2AD). The control signal was sent to the machine tool PLC (Programmable Logic Controller) at a frequency of 50 Hz to update the machining feedrate of the machine tool, when the spindle load was changed. The parameters of the controller were fixed while the feedrates were real-time updated.

### E. PROCESSES OF END AND SLOT MILLING

A medium carbon steel S45C was used for the milling experiments. The cutting tool used was a 2.0 mm diameter two-flute end mill without surface coating (AA238M-0200-D4-ML-10) produced by Jingming Precision Tools (Taiwan) as shown in Figure 2(d). The tool material was composed by 0.4  $\mu\text{m}$  ultra-fine grained tungsten carbide particles (WC88%, Co12%). Length of cut was 5.0 mm. The helix angle was 38°, axial primary relief angle was 3°, and the hardness value was 55 HRC. The machining length of each pass was 150 mm, and the axial depth was 200  $\mu\text{m}$ . End and slot milling experiments were performed at the spindle speed of 10000 rpm. The radial machining depth of end milling was 1.4 mm (70% of the tool diameter), and the down-milling operation was chosen for end milling tests. In the constant feed experiment, the spindle load current of each machining test and the flank wear at the end of the machining tests were recorded. In the

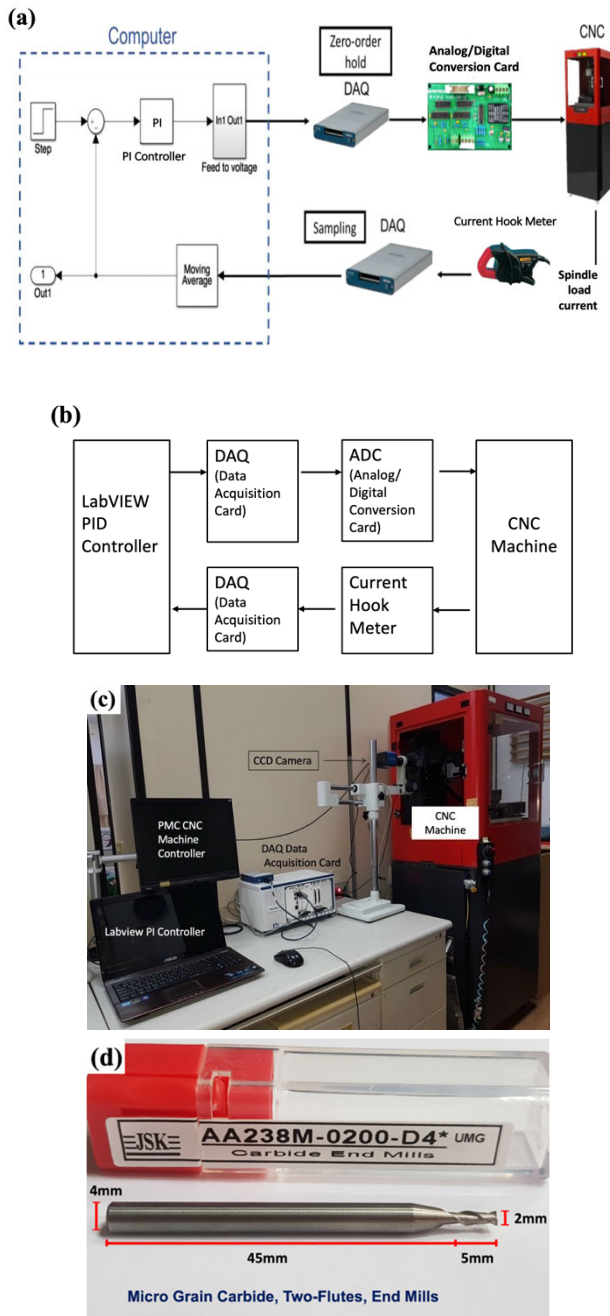


**FIGURE 2.** The equipment of the control system: (a) overview, (b) architecture diagram, (c) main interfaces, (d) cutting tool.

constant load machining test, each machining test's feedrate, spindle load current, and flank wear were recorded.

**F. PARAMETERS SETTING**

In constant load milling, the spindle current was maintained at the reference current level, and the feedrate was updated according to the reference current. The reference current and the upper limit of the feedrate were set based on the strength of the cutting tool and surface roughness. The lower limit of the feedrate was based on the tool wear amount. When the feedrate reached the lower limit, the cutting force resulted

from material removal and tool wear was expected to be close to the upper limit that the cutting tool can withstand. In addition, the tool wear value was expected to be maintained within the range predetermined in this study. The following steps were used to set the spindle reference current, feedrate upper limit, and feedrate lower limit for constant load milling:

1) The maximum spindle current that the tool can bear was obtained from the constant feed milling tests, and a safety factor was added to set the spindle reference current.

2) From the relationship between the feedrate and the spindle current, the initial feedrate corresponding to the reference current was obtained.

3) The lower limit of feedrate was determined according to (15).  $f_m$  was the lower limit of feedrate when  $V_B$  reaches the maximum. The lower limit of feedrate was also set referring to the constant feedrate milling tests when the tool was severely worn and starts to produce unstable wear, such as chipping. This must be done with a series of constant feedrate milling tests.

After the processing parameters were formulated, the PI controller parameters would be designed and verified. The PI controller was mainly to stabilize the spindle current. Then the previously set constant load processing parameters would be verified experimentally to determine whether a stable milling process can be achieved. It would also be examined in the experiments if the tool wear remained within the selected range, which was the time to change the tool when the feedrate reached the lower limit.

**G. FLANK WEAR MEASUREMENT**

The method of measuring flank wear was to use a CCD Camera (SAGE VISION HD4600) to capture the image of the tool end face and estimated the maximum flank wear on each edge of the end face. The averages of the maximum wear of the two tool end faces were recorded. By observing the tool condition in milling tests, when the wear value of the tool used in this experiment was around  $220 \mu\text{m}$  to  $230 \mu\text{m}$ , an unstable wear phenomenon began to appear. Therefore, the maximum tool wear in this study was set as  $180 \mu\text{m}$  to  $220 \mu\text{m}$  to prevent unstable tool wear or chipping.

**H. SYSTEM IDENTIFICATION**

This study used the chirp signals for system identification [40] to identify the machining system dynamics. The PI controller for constant load milling was designed based on the machining system dynamics. This study used LabVIEW [39] to create the chirp signals and the block diagram of the program is shown in Figure 3, where  $f_1$  and  $f_2$  were the start and end frequencies of the chirp signals, respectively. The input signal was the voltage signal for controlling the feedrate. The output signal of the CNC was the spindle current. After getting the input and output signals, the ARX Model of MATLAB [41], [42] was used to identify the dynamic equation between input and output signals. In the PI controller design, the proper ratio gain  $K_p$ , and integral gain  $K_i$  were set by the

PID Tuner module of MATLAB Simulink as the parameters for constant load milling. For system identification, a new tool was used, the spindle speed was 10000 rpm, and the axial depth of cut was 0.2 mm for slot and end milling. In the experiments of slot and end milling, the feedrates ranged from 250 to 750 mm/min.

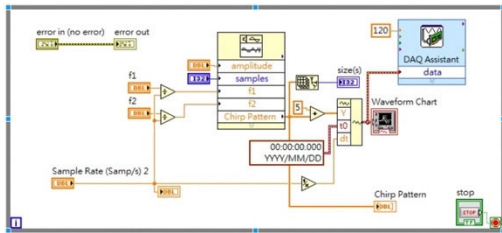


FIGURE 3. Chirp signal block diagram.

### III. EXPERIMENTAL RESULTS

#### A. PARAMETER SETTING BY CONSTANT FEEDRATE

##### 1) END MILLING

The relationship between the feedrates and spindle current of sharp cutters for end milling is shown in Figure 4. Three cutting tests were carried out for each cutting condition. The relationship between feedrate and current was linear and can be estimated by (13).

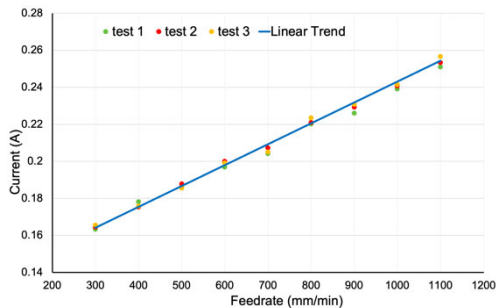


FIGURE 4. The relationship between the feedrate of the new tool for end milling and the spindle current.

In the tool wear experiments of end milling with constant feedrates of 800, 900, and 1000 mm/min, the spindle current of these three feedrates were significantly increased when the spindle current exceeded 0.28A, as shown in Figure 5. The spindle current of 1000 mm/min feedrate was sharply raised to 0.298A at the end of the cutting test, and the chipping was observed, as shown in Figure 6. According to the experimental results, the maximum spindle current that the worn tool can withstand was about 0.28 A. For safety reasons, we set a safety factor of 1.17 to avoid unpredictable tool failure. The spindle reference current was set to 0.24A by multiplying the maximum spindle current of 0.28A by 0.85. In Figure 4, the feedrate corresponding to the initial spindle current of 0.24 A without any tool wear was about 1000 mm/min. Therefore, the upper limit of the feedrate for end milling was set to 1000 mm/min. If the spindle current exceeds the upper limit, the feedrate will decrease immediately to avoid tool chipping or breakage.

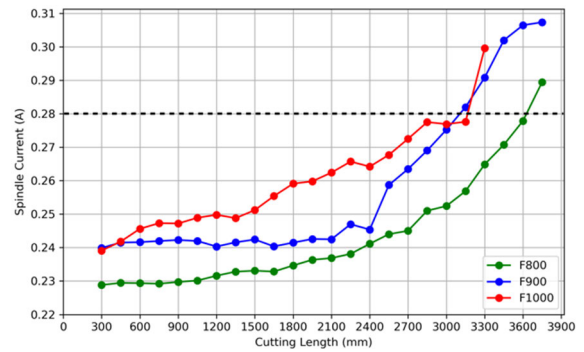


FIGURE 5. Spindle current of end milling with three constant feedrates (800, 900, and 1000 mm/min).

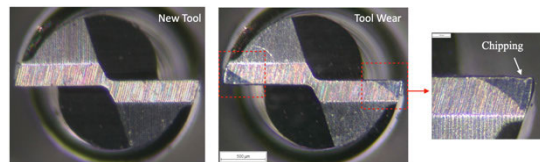


FIGURE 6. Flank wear of end milling with constant feedrate (1000 mm/min) when the current rises to 0.298 A.

The wear experiments for the lower limit of the feedrate are shown in Figure 7. The experiments were carried out at feedrates of 600 and 700 mm/min. When the spindle current at the feedrate of 700 mm/min was close to the reference current of 0.24 A, the flank wear was 167.3  $\mu\text{m}$ , lower than the desired wear range of 180  $\mu\text{m}$ -220  $\mu\text{m}$ . As a result, if 700 mm/min was set as the lower limit of the feedrate, the tool wear may not enter the preset tool change range at the end of the milling experiment. When the spindle current at a feedrate of 600 mm/min reached 0.236 A, the tool wear was 205.1  $\mu\text{m}$ , which was in the middle of the wear range of 180  $\mu\text{m}$ -220  $\mu\text{m}$ . Therefore, setting 600 mm/min as the lower limit of the feedrate would be appropriate.

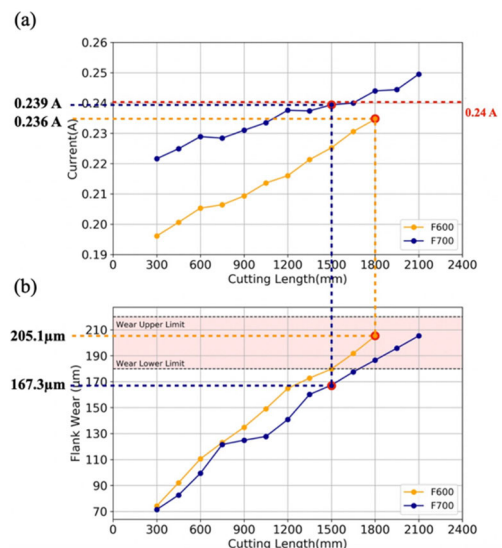


FIGURE 7. Constant feedrate end milling of 600 and 700 mm/min.

2) SLOT MILLING

The process of selecting processing parameters for constant-load slot milling is the same as end milling. The relationship between feedrate in slot milling and spindle current for sharp cutting tools is shown in Figure 8. The same condition was tested three times. The relationship of feedrate and current in slot milling was also linear.

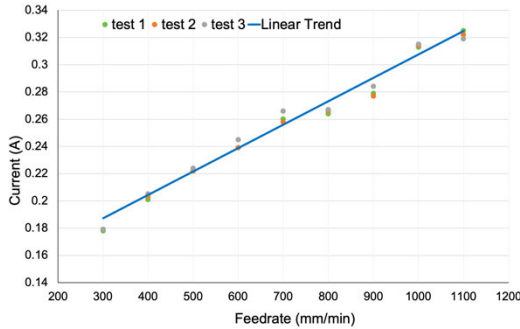


FIGURE 8. The relationship between slot milling feedrate and spindle current.

A set of constant feedrate experiments from 400 mm/min to 800 mm/min were carried out every 100 mm/min to record the spindle current and tool wear status. The experimental results showed that when the feedrate was 800 mm/min, the spindle current reached 0.282 A and began to produce chipping. Therefore, the highest spindle current that the tool can withstand after tool wear is about 0.28 A, which was coincidentally the same as the maximum current in end milling. Same as in end milling, a safety factor of 1.17 was set for the spindle reference current to reduce the risk of chipping or tool breakage during cutting tests. Then, the maximum spindle current of 0.28A was multiplied by 0.85 to obtain the reference current of 0.24A.

According to the experimental results in Figure 8, the feedrate corresponding to the reference current of 0.24 A was 600 mm/min. To improve the machining efficiency, the upper limit of the feedrate for slot milling was slightly increased to 700 mm/min.

Slot milling wear experiments were conducted with feedrates of 400 and 500 mm/min and recorded the average spindle current and the tool wear status at the end of each cut. When the spindle current reached the reference current 0.24 A at the feedrate of 500 mm/min, the tool wear was about 180~190 μm, located at the lower edge of the tool change interval 180 μm – 220 μm. It was a slightly conservative but reasonable lower feedrate setting value. Therefore, the lower limit of feedrate for slot milling in this study was set at 500 mm/min.

B. VERIFICATION OF CONSTANT LOAD CONTROL

1) END MILLING

Before the design of the PI controller, the dynamics of the machining system are determined by the sine-swept method.

The formula of the chirp sine signal is as follows:

$$y = A \times \sin \left( 2\pi \left( f_0 + \frac{f_1 - f_0}{2T_e} \times T_i \right) T_i \right) \quad (17)$$

where A is the intensity, f<sub>0</sub> is the initial frequency, f<sub>1</sub> is the end frequency, T<sub>e</sub> is the target time, T<sub>i</sub> is the instantly time, and y is the output waveform.

In this study, the intensity was 2.5 V, the target time was 15 seconds, and the frequency was increased from 0.1 Hz to 2 Hz. Observing the system’s response to the input signal, and using the MATLAB to obtain the transfer function that best fits the system’s dynamic characteristics, the transfer function between the feedrate input voltage and the spindle current output was obtained as follows:

$$G_{cnc} = \frac{0.0611z^{-1} - 0.1338z^{-2} + 0.0752z^{-3}}{1 - 2.0311z^{-1} + 1.2104z^{-2} - 0.1655z^{-3}} \quad (18)$$

G<sub>CNC</sub> is the transfer function of the machining system. After obtaining the transfer function of the machining system, the proportional gain and integral gain that meet the system response requirements were estimated through MATLAB. According to the experimental results, the K<sub>p</sub> of the PI controller was set to 160, K<sub>i</sub> was set to 0.006, where the rising time was set to 2 seconds, the settling time was set to 4 seconds, and the settling error was set to 0. An example of the control signal for constant load end milling (cutting length = 150~300mm) is shown in Figure 9. The reference current was set to 0.24 A, and the average of the measured current was 0.239 A. The difference between maximum and minimum current during end milling was 7.6%.

The end milling parameters established for the constant load machining process were set to the reference spindle current of 0.24A, the upper limit of the feedrate to be 1000mm/min, and the lower limit of the feed speed to be 600mm/min. When the feedrate reached the lower limit in cutting tests, the controller could not continue to reduce the feedrate, as shown in Figure 10. The relationships of spindle current and feedrate (5 different tests in the same condition) to cutting lengths are shown in Figure 11. The current was successfully controlled within 1% of the reference current before the feedrate reached the lower limit. Despite the slightly different properties of the tools, reflecting in changes of feedrates during cutting tests, the proposed method always recommended the proper tool changing time and proved to avoid severe tool damage.

2) SLOT MILLING

The process to obtain the transfer function of the cutting system of slot milling is similar to that of end milling. According to the experimental results, the K<sub>p</sub> of the PI controller was set to 160, K<sub>i</sub> was set to 0.006, where the rising time was set to 2 seconds, settling time was set to 4 seconds and the settling error was set to 0. The experimental results of applying PI controller parameters to constant load machining (cutting length = 150~300mm) is shown in Figure 12. The reference current was 0.24 A, while the actual processing

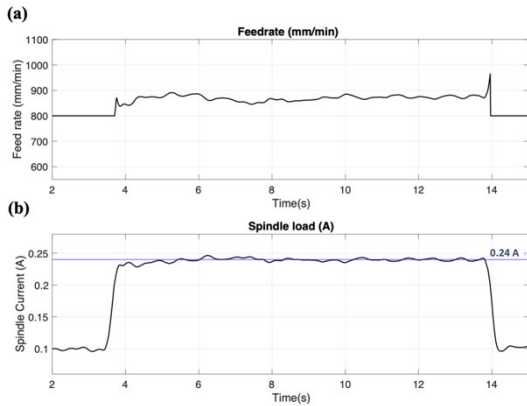


FIGURE 9. Control effect of constant load end milling.

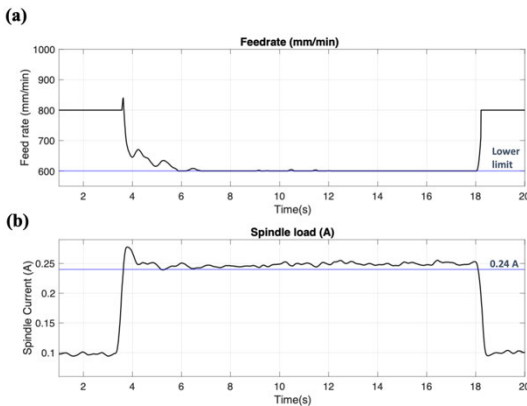


FIGURE 10. Constant load end milling when the feedrate reached the lower limit (a) feedrate (b) spindle current (cutting length = 2000~2400mm).

End milling

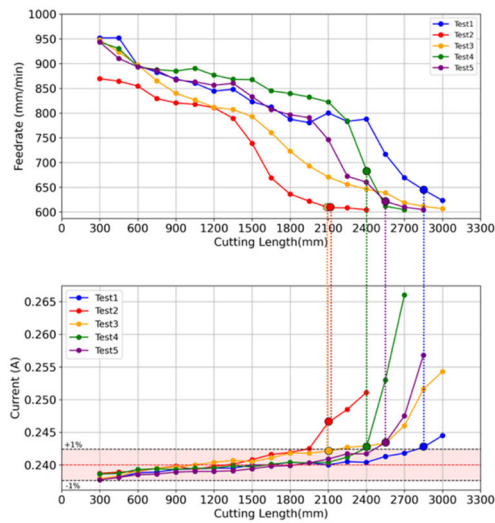


FIGURE 11. Spindle current and feedrate of constant load end milling.

average current was controlled at 0.240 A. The difference between maximum and minimum current during processing was 7.5%.

The machining parameters established in the constant load machining process were set to the current of 0.24A, the upper limit of the feedrate to 700mm/min, and the lower limit of the feedrate to 500mm/min. The spindle current rose when the feedrate dropped to the lower limit (cutting length = 1500~2000mm, as shown in Figure 13). The relationships of the average spindle current and feedrate to cutting lengths for constant load machining (3 tests in the same condition) are shown in Figure 14. The current was successfully controlled within 1% of the reference current before the feedrate reached the lower limit. The proposed method always recommended the proper tool changing time and proved to avoid severe tool damage. The red line (test1) shows that the feedrate is higher in the initial machining stage, but the spindle current still maintains an error of  $\pm 1\%$ . This was because the origin of the Z axis was manually set, which caused a smaller depth of cut and as a result of a higher feedrate during constant load milling in test 1.

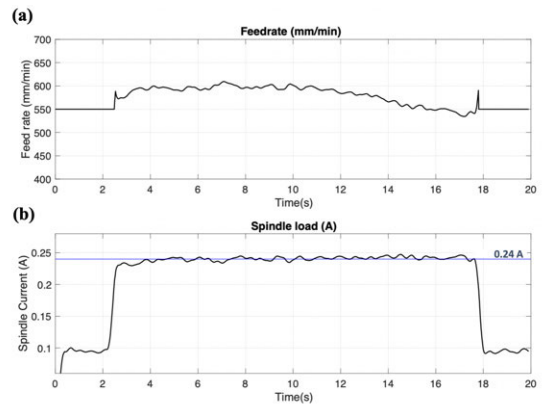


FIGURE 12. Control effect of constant load machining slot milling processing (a) Feedrate (b) Spindle current.

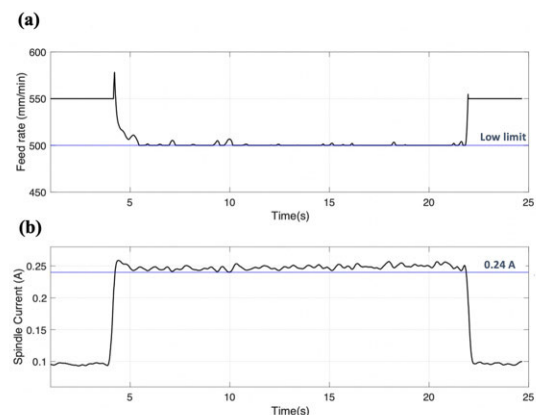


FIGURE 13. Constant load slot milling when the feedrate reached the lower limit (a) feedrate (b) spindle current.

### C. VERIFICATION OF TOOL CHANGE TIMING

#### 1) END MILLING

The progresses of flank wear are shown in Figure 15, where the feedrate were almost falling to the lower limit at the end of cutting tests. Table 1 summarizes the flank wear measured



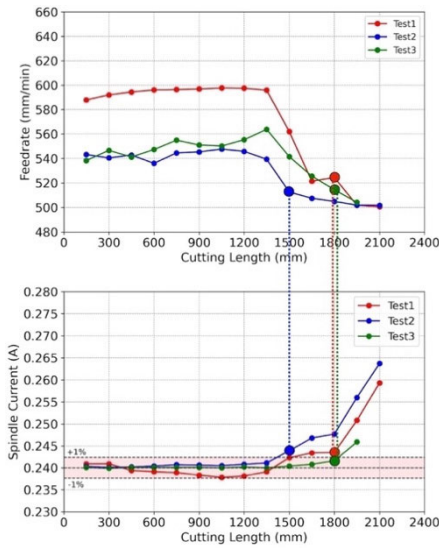


FIGURE 14. Spindle current and feedrate of constant load slot milling.

at the end of cutting tests when the feedrate reached the lower limit. The results showed that when the feedrate reached the lower limit, the tool wear did not exceed the upper limit of the tool change interval. The average value was  $197.26 \mu\text{m}$ , approximately in the middle of the tool change interval. It is observed in the figure that when the tool wear fell within the preset range, the total cutting lengths differed. Compared with the traditional method, which estimated tool life by cutting lengths, the proposed method can accurately predict the timing of tool change. The traditional method estimated tool life by cutting lengths. Based on the characteristics of constant load machining, the feedrate needs to be decreased as the tool wear increases. We set a lower limit of feedrate to reflect the tool wear status. When the feedrate command touched the lower limit, it is indicated that the tool wear reaches its limit and it needs to be replaced. This method works better than the traditional method if there are variations among cutting tool properties, where estimating tool life by cutting length does not work well.

TABLE 1. Flank wear results when the feedrate of constant load end milling reaches the lower limit.

Test	The tool wear value ( $\mu\text{m}$ ) (When the feedrate reached the lower limit.)	The tool wear value location
1	214.30	Locate in the tool change interval
2	175.29	4.71 $\mu\text{m}$ Lower than the lower limit of interval
3	192.34	Locate in the tool change interval
4	198.59	Locate in the tool change interval
5	205.80	Locate in the tool change interval
Average	197.26	

2) SLOT MILLING

The progresses of flank wear for constant load slot milling are shown in Figure 16. Tool wear values measured at the end of machining when the feedrate reached the lower limit were summarized in Table 2. The results showed that when the

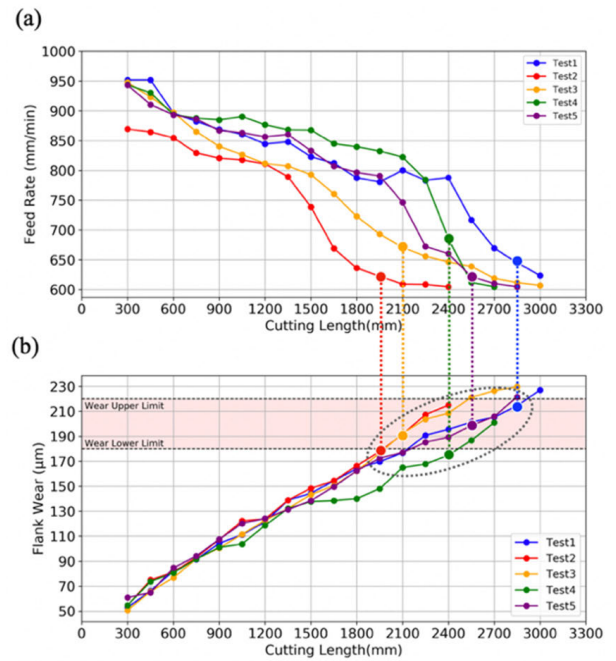


FIGURE 15. Constant load end milling (a) Feedrate (b) flank wear.

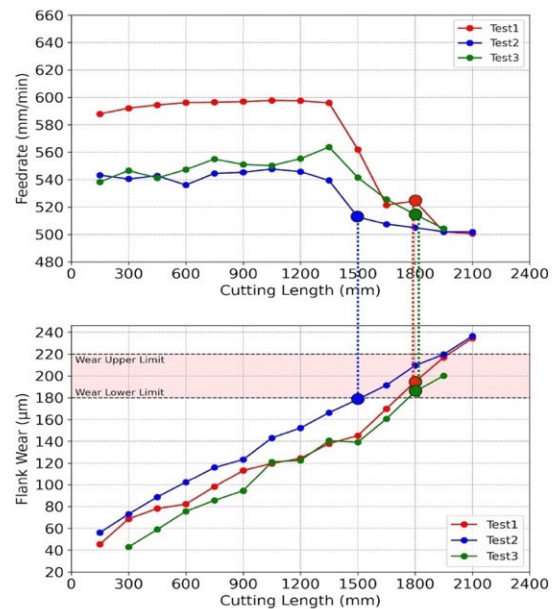


FIGURE 16. Constant load slot milling (a) Feedrate (b) flank wear.

feedrate reached the lower limit, the tool wear did not exceed the upper limit of the tool change interval. The average value was  $189.70 \mu\text{m}$ , within the range of  $180 \mu\text{m}$  to  $220 \mu\text{m}$ .

D. MATERIAL REMOVAL RATE AND TOOL LIFE

1) END MILLING

The comparison of tool wear performance between constant load machining and traditional constant feedrate machining is shown in Figure 17 (test1 to test5 were the results of constant load machining). Because the spindle load current was unstable during constant feedrate machining with  $800 \text{ mm/min}$ ,

**TABLE 2.** The results of tool web wear when the feedrate of constant load slot milling reaches the lower limit.

Test	The tool wear value ( $\mu\text{m}$ ) (When the feedrate reached the lower limit.)	The tool wear value location
1	194.53	Locate in the tool change interval
2	178.89	1.11 $\mu\text{m}$ Lower than the lower limit of interval
3	195.69	Locate in the tool change interval
Average	189.70	

as shown in Figure 18 (a) and the chipping phenomenon was observed as shown in Figure 18 (b), only the experimental results for constant feedrate machining of 700 mm/min and 600 mm/min were compared.

As shown in Figure 17, the average tool life of constant load end milling was 2250 mm, and the tool life of constant feedrate of 700 mm/min was 1800 mm. Constant load machining has a 25% increase in tool life. The material removal rate (MRR) for constant load end milling was 3.79 mm<sup>3</sup>/s, while the MRR for constant feedrate 700 mm/min was 3.26 mm<sup>3</sup>/s. There was a 16% increase in material removal rate for constant load milling. The results are as expected, because most of the time, the feedrate of constant load machining was higher than that of constant feedrate machining.

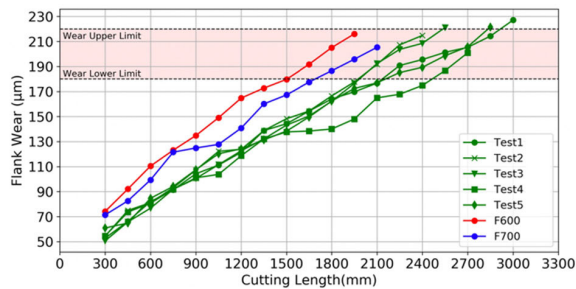


**FIGURE 17.** Comparison of flank wear between constant feedrate (F600, F700) and constant load end milling (5 tests).

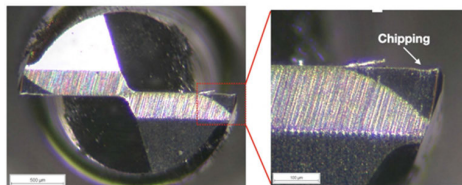
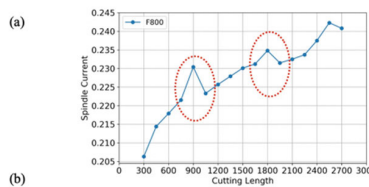


**FIGURE 18.** (a) Spindle current at constant feedrate end milling of 800 mm/min, (b) Tool chipping phenomenon at constant feedrate of 800 mm/min.

## 2) SLOT MILLING

Referring to the processing parameters recommended by the tool manufacturer, this study compared the flank wear

progress of constant feedrate 400 mm/min and constant load slot milling, as shown in Figure 19. The results showed that the tool life of constant load machining was longer than that of traditional slot milling recommended by tool manufacturers. The average material removal rate for constant load processing was 3.93 mm<sup>3</sup>/s, and the total cutting length was 1950 mm. The average material removal rate for constant feedrate machining was 2.53 mm<sup>3</sup>/s, and the total cutting length was 1350 mm. Constant load machining has a 44% increase in tool life. There was a 55% increase in material removal rate for constant load milling.

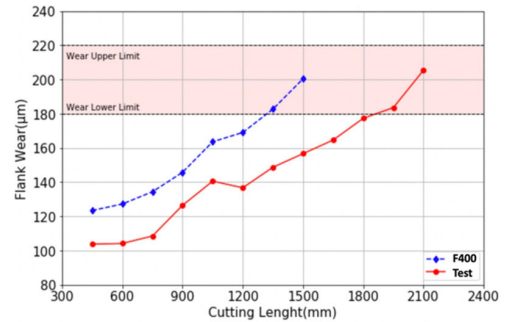


**FIGURE 19.** Comparison of flank wear between constant feedrate 400mm/min and constant load slot milling (Test).

## E. CONSTANT LOAD MACHINING IN HYBRID SLOT AND END MILLING

The tool paths for a simple microfluidic mold are shown in Figure 20(a). The designed tool paths were a mixed processing of slot and end milling, as shown in Figure 20 (b). The machining parameters of constant load slot milling and end milling were shown in Table 3.

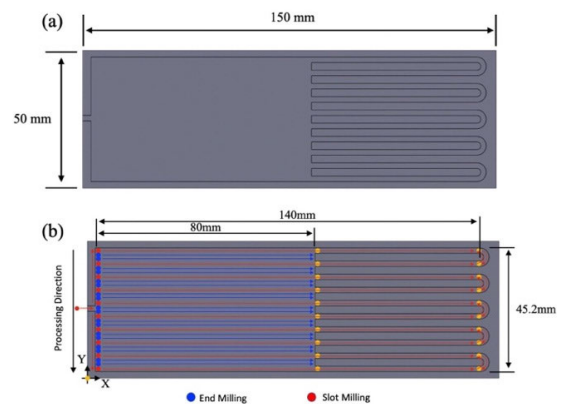


**FIGURE 20.** (a) Machining geometry, (b) Machining length and tool path.

**TABLE 3.** Parameters for geometry machining.

	Slot Milling	End Milling
Spindle Reference Current (A)	0.24	0.24
Upper Limit of Feedrate (mm/min)	700	1100
Lower Limit of Feedrate (mm/min)	500	600

Machining experiments were carried out on two workpieces. In the two experiments, the feedrate reached the lower

limit of feedrate at different locations for the first cutting tool, as shown in Figure 21(a). The feedrate and spindle current signals are shown in Figure 22 (a)~(d). The values of tool flank wear were  $179.48 \mu\text{m}$  and  $199.63 \mu\text{m}$ , located in the tool change interval region. In the two experiments. After the feedrate reached the lower limit, the wear amount could still be kept lower than  $220 \mu\text{m}$  until the end of the cut, and then the tool was changed to finish the processing. The finished product is shown in Figure 21(b). The two workpieces were successfully made without defects caused by excessive tool wear.

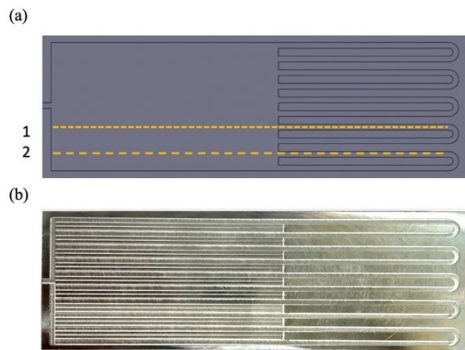


**FIGURE 21.** (a) The processing pass when the feedrate reaches the lower limit in two machining verification experiments, (b) The finished product of the image of geometry machining verification experiment.

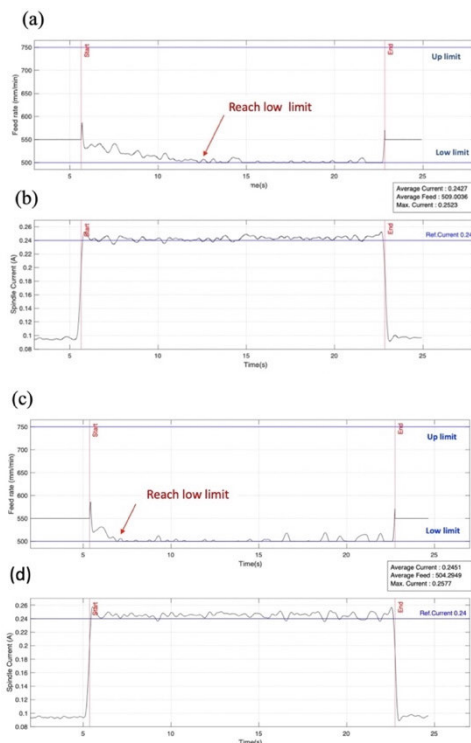


**FIGURE 22.** Processing signal before tool change in second machining verification experiment (a), (c) Feedrate; (b), (d) Spindle current.

#### IV. CONCLUSION

This work proposes a systematic parameter-setting strategy for constant load machining. Constant feedrate experiments

can be used to determine parameters such as spindle reference current, upper limit of feedrate, and lower limit of feedrate. The spindle current and feedrate are set based on the tool strength and tool wear characteristics by understanding the relationship between tool wear, spindle current, and feedrate. The suggested process parameters for constant load machining can reflect changes in tool wear and feedrate during the machining process. The tool wear falls within the defined range of tool wear when the feedrate hits the lower limit. The proposed solution allows the process parameters to be established systematically without random guesses. When compared to the manufacturer's recommended machining parameters, tool life and material removal rates are effective and good. Constant load machining increased tool life by 23% and material removal rate by 16% for end milling. Constant load machining improves material removal rate by 51% and tool life by 30% in slot milling. This research also established the viability of using constant load machining on a mixed path of slot and end milling.

The machining process is often complex. If we want to dynamically adjust the feedrate to keep a constant spindle current, we need a reference current. In this study, we proposed a methodology to find the reference current, the upper and lower limit feedrate for different tools without random guesses. Compared to traditional method of parameter identification, i.e., random guesses, the advantages of the proposed methodology can guarantee better machining efficiency than machining with fixed feedrates.

#### REFERENCES

- [1] R. G. Landers, K. Barton, S. Devasia, T. Kurfess, P. Pagilla, and M. Tomizuka, "A review of manufacturing process control," *J. Manuf. Sci. Eng.*, vol. 142, no. 11, Nov. 2020, Art. no. 110814, doi: 10.1115/1.4048111.
- [2] A. Mohamed, M. Hassan, R. M'Saoubi, and H. Attia, "Tool condition monitoring for high-performance machining systems—A review," *Sensors*, vol. 22, no. 6, p. 2206, Mar. 2022, doi: 10.3390/s22062206.
- [3] F. I. Compeán, D. Olvera, F. J. Campa, L. N. L. De Lacalle, A. Elías-Zúñiga, and C. A. Rodríguez, "Characterization and stability analysis of a multivariable milling tool by the enhanced multistage homotopy perturbation method," *Int. J. Mach. Tools Manuf.*, vol. 57, pp. 27–33, Jun. 2012, doi: 10.1016/j.ijmactools.2012.01.010.
- [4] G. Urbikain, L. N. L. De Lacalle, and A. Fernández, "Regenerative vibration avoidance due to tool tangential dynamics in interrupted turning operations," *J. Sound Vib.*, vol. 333, no. 17, pp. 3996–4006, Aug. 2014, doi: 10.1016/j.jsv.2014.03.028.
- [5] M. Ghobakhloo, "Industry 4.0, digitization, and opportunities for sustainability," *J. Cleaner Prod.*, vol. 252, Apr. 2020, Art. no. 119869, doi: 10.1016/j.jclepro.2019.119869.
- [6] M.-Q. Tran, H.-P. Doan, V. Q. Vu, and L. T. Vu, "Machine learning and IoT-based approach for tool condition monitoring: A review and future prospects," *Measurement*, vol. 207, Feb. 2023, Art. no. 112351, doi: 10.1016/j.measurement.2022.112351.
- [7] B. Siddhartha, A. P. Chavan, K. H. Gopala, and K. N. Subramanya, "IoT enabled real-time availability and condition monitoring of CNC machines," in *Proc. IEEE Int. Conf. Internet Things Intell. Syst. (IoT&IS)*, Jan. 2021, pp. 78–84, doi: 10.1109/IoT&IS50849.2021.9359698.
- [8] Y. Koren, "Adaptive control systems for machining," in *Proc. Amer. Control Conf.*, Jun. 1988, pp. 1161–1167.
- [9] L. K. Lauderbaugh and A. G. Ulsoy, "Dynamic modeling for control of the milling process," *J. Eng. Ind.*, vol. 110, no. 4, pp. 367–375, Nov. 1988, doi: 10.1115/1.3187896.

- [10] A. G. Ulsoy, Y. Koren, and F. Rasmussen, "Principal developments in the adaptive control of machine tools," *J. Dyn. Syst., Meas., Control*, vol. 105, no. 2, pp. 107–112, Jun. 1983, doi: [10.1115/1.3149640](https://doi.org/10.1115/1.3149640).
- [11] B. K. Fussell and K. Srinivasan, "Model reference adaptive control of force in end milling operations," in *Proc. Amer. Control Conf.*, Jun. 1988, pp. 1189–1194, doi: [10.23919/ACC.1988.4789901](https://doi.org/10.23919/ACC.1988.4789901).
- [12] Y. Liu, T. Cheng, and L. Zuo, "Adaptive control constraint of machining processes," *Int. J. Adv. Manuf. Technol.*, vol. 17, no. 10, pp. 720–726, May 2001, doi: [10.1007/s001700170117](https://doi.org/10.1007/s001700170117).
- [13] Y. Liu and C. Wang, "Neural network based adaptive control and optimization in the milling process," *Int. J. Adv. Manuf. Technol.*, vol. 15, no. 11, pp. 791–795, Oct. 1999, doi: [10.1007/s001700050133](https://doi.org/10.1007/s001700050133).
- [14] M.-Y. Yang, T.-M. Lee, and J.-G. Choi, "A new spindle current regulation algorithm for the CNC end milling process," *Int. J. Adv. Manuf. Technol.*, vol. 19, no. 7, pp. 473–481, Apr. 2002, doi: [10.1007/s001700200050](https://doi.org/10.1007/s001700200050).
- [15] M.-Y. Yang and T.-M. Lee, "Hybrid adaptive control based on the characteristics of CNC end milling," *Int. J. Mach. Tools Manuf.*, vol. 42, no. 4, pp. 489–499, Mar. 2002, doi: [10.1016/S0890-6955\(01\)00138-9](https://doi.org/10.1016/S0890-6955(01)00138-9).
- [16] T. Mohanraj, S. Shankar, R. Rajasekar, N. R. Sakthivel, and A. Pramanik, "Tool condition monitoring techniques in milling process—A review," *J. Mater. Res. Technol.*, vol. 9, no. 1, pp. 1032–1042, Jan. 2020, doi: [10.1016/j.jmrt.2019.10.031](https://doi.org/10.1016/j.jmrt.2019.10.031).
- [17] Z. Huang, J. Zhu, J. Lei, X. Li, and F. Tian, "Tool wear predicting based on multi-domain feature fusion by deep convolutional neural network in milling operations," *J. Intell. Manuf.*, vol. 31, no. 4, pp. 953–966, Apr. 2020, doi: [10.1007/s10845-019-01488-7](https://doi.org/10.1007/s10845-019-01488-7).
- [18] G. Urbikain and L. N. L. De Lacalle, "MoniThor: A complete monitoring tool for machining data acquisition based on FPGA programming," *SoftwareX*, vol. 11, Jan. 2020, Art. no. 100387, doi: [10.1016/j.softx.2019.100387](https://doi.org/10.1016/j.softx.2019.100387).
- [19] L. N. L. de Lacalle, A. Lamikiz, J. A. Sanchez, and I. F. de Bustos, "Simultaneous measurement of forces and machine tool position for diagnostic of machining tests," *IEEE Trans. Instrum. Meas.*, vol. 54, no. 6, pp. 2329–2335, Dec. 2005, doi: [10.1109/TIM.2005.858535](https://doi.org/10.1109/TIM.2005.858535).
- [20] L. N. L. D. Lacalle, A. Lamikiz, J. A. Sánchez, and I. F. D. Bustos, "Recording of real cutting forces along the milling of complex parts," *Mechatronics*, vol. 16, no. 1, pp. 21–32, Feb. 2006, doi: [10.1016/j.mechatronics.2005.09.001](https://doi.org/10.1016/j.mechatronics.2005.09.001).
- [21] T. Mohanraj, J. Yechuru, H. Krishnan, R. S. N. Aravind, and R. Yameni, "Development of tool condition monitoring system in end milling process using wavelet features and Hoelder's exponent with machine learning algorithms," *Measurement*, vol. 173, Mar. 2021, Art. no. 108671, doi: [10.1016/j.measurement.2020.108671](https://doi.org/10.1016/j.measurement.2020.108671).
- [22] S. Roy and B. Das, "An appliance of adaptive neuro-fuzzy inference system for predicting the surface roughness of Al-4.5%Cu-TiC MMC in turning operation of CNC milling," *Mater. Today, Proc.*, vol. 62, pp. 3749–3755, Jan. 2022, doi: [10.1016/j.matpr.2022.04.449](https://doi.org/10.1016/j.matpr.2022.04.449).
- [23] K. B. Radha, V. Ramesh, S. C. Mathalai, T. R. Theerka, and A. K. L. Madan, "Analyse the surface quality in the milling process by soft computing approaches," *Mater. Today, Proc.*, vol. 69, pp. 1462–1464, Jan. 2022, doi: [10.1016/j.matpr.2022.09.598](https://doi.org/10.1016/j.matpr.2022.09.598).
- [24] J. Yuan, L. Liu, Z. Yang, J. Bo, and Y. Zhang, "Tool wear condition monitoring by combining spindle motor current signal analysis and machined surface image processing," *Int. J. Adv. Manuf. Technol.*, vol. 116, nos. 7–8, pp. 2697–2709, Oct. 2021, doi: [10.1007/s00170-021-07366-y](https://doi.org/10.1007/s00170-021-07366-y).
- [25] I. Zamudio-Ramírez, J. A. Antonino-Daviu, M. Trejo-Hernandez, and R. A. Osornio-Rios, "Cutting tool wear monitoring in CNC machines based in spindle-motor stray flux signals," *IEEE Trans. Ind. Informat.*, vol. 18, no. 5, pp. 3267–3275, May 2022, doi: [10.1109/TII.2020.3022677](https://doi.org/10.1109/TII.2020.3022677).
- [26] Y. Zhou and W. Sun, "Tool wear condition monitoring in milling process based on current sensors," *IEEE Access*, vol. 8, pp. 95491–95502, 2020, doi: [10.1109/ACCESS.2020.2995586](https://doi.org/10.1109/ACCESS.2020.2995586).
- [27] K.-J. Lee, T.-M. Lee, and M.-Y. Yang, "Tool wear monitoring system for CNC end milling using a hybrid approach to cutting force regulation," *Int. J. Adv. Manuf. Technol.*, vol. 32, nos. 1–2, pp. 8–17, Feb. 2007, doi: [10.1007/s00170-005-0350-0](https://doi.org/10.1007/s00170-005-0350-0).
- [28] D. Kim and D. Jeon, "Fuzzy-logic control of cutting forces in CNC milling processes using motor currents as indirect force sensors," *Precis. Eng.*, vol. 35, no. 1, pp. 143–152, Jan. 2011, doi: [10.1016/j.precisioneng.2010.09.001](https://doi.org/10.1016/j.precisioneng.2010.09.001).
- [29] J. Tlustý and M. A. A. Elbestawi, "Analysis of transients in an adaptive control servomechanism for milling with constant force," *J. Eng. Ind.*, vol. 99, no. 3, pp. 766–772, Aug. 1977, doi: [10.1115/1.3439311](https://doi.org/10.1115/1.3439311).
- [30] C. C. Lee, "Fuzzy logic in control systems: Fuzzy logic controller. I," *IEEE Trans. Syst., Man, Cybern.*, vol. 20, no. 2, pp. 404–418, Mar./Apr. 1990, doi: [10.1109/21.52551](https://doi.org/10.1109/21.52551).
- [31] C. Xu and Y. C. Shin, "An adaptive fuzzy controller for constant cutting force in end-milling processes," *J. Manuf. Sci. Eng.*, vol. 130, no. 3, Jun. 2008, Art. no. 031001, doi: [10.1115/1.2823070](https://doi.org/10.1115/1.2823070).
- [32] D. R. Salgado and F. J. Alonso, "An approach based on current and sound signals for in-process tool wear monitoring," *Int. J. Mach. Tools Manuf.*, vol. 47, no. 14, pp. 2140–2152, Nov. 2007, doi: [10.1016/j.ijmactools.2007.04.013](https://doi.org/10.1016/j.ijmactools.2007.04.013).
- [33] U. Zuperl, F. Cus, and M. Reibenschuh, "Neural control strategy of constant cutting force system in end milling," *Robot. Comput.-Integr. Manuf.*, vol. 27, no. 3, pp. 485–493, Jun. 2011, doi: [10.1016/j.rcim.2010.10.001](https://doi.org/10.1016/j.rcim.2010.10.001).
- [34] Y. Altintas, "Prediction of cutting forces and tool breakage in milling from feed drive current measurements," *J. Eng. Ind.*, vol. 114, no. 4, pp. 386–392, Nov. 1992, doi: [10.1115/1.2900688](https://doi.org/10.1115/1.2900688).
- [35] S. Kim and S. Chung, "Cutting force estimation using feeddrive and spindle motor currents in milling processes," *Trans. KSME A*, vol. 22, no. 11, pp. 2029–2038, 1998.
- [36] J.-G. Choi and M.-Y. Yang, "In-process prediction of cutting depths in end milling," *Int. J. Mach. Tools Manuf.*, vol. 39, no. 5, pp. 705–721, May 1999, doi: [10.1016/S0890-6955\(98\)00067-4](https://doi.org/10.1016/S0890-6955(98)00067-4).
- [37] R. P. Borase, D. K. Maghade, S. Y. Sondkar, and S. N. Pawar, "A review of PID control, tuning methods and applications," *Int. J. Dyn. Control*, vol. 9, no. 2, pp. 818–827, Jun. 2021, doi: [10.1007/s40435-020-00665-4](https://doi.org/10.1007/s40435-020-00665-4).
- [38] R. A. Osornio-Rios, R. D. J. Romero-Troncoso, G. Herrera-Ruiz, and R. Castañeda-Miranda, "The application of reconfigurable logic to high speed CNC milling machines controllers," *Control Eng. Pract.*, vol. 16, no. 6, pp. 674–684, Jun. 2008, doi: [10.1016/j.conengprac.2007.08.004](https://doi.org/10.1016/j.conengprac.2007.08.004).
- [39] M. A. K. Alia, T. M. Younes, and S. A. Subah, "A design of a PID self-tuning controller using LabVIEW," *J. Softw. Eng. Appl.*, vol. 4, no. 3, pp. 161–171, Mar. 2011, doi: [10.4236/jsea.2011.43018](https://doi.org/10.4236/jsea.2011.43018).
- [40] X.-G. Xia, "System identification using chirp signals and time-variant filters in the joint time-frequency domain," *IEEE Trans. Signal Process.*, vol. 45, no. 8, pp. 2072–2084, Aug. 1997, doi: [10.1109/78.611210](https://doi.org/10.1109/78.611210).
- [41] H. Ohlsson, L. Ljung, and S. Boyd, "Segmentation of ARX-models using sum-of-norms regularization," *Automatica*, vol. 46, no. 6, pp. 1107–1111, Jun. 2010, doi: [10.1016/j.automatica.2010.03.013](https://doi.org/10.1016/j.automatica.2010.03.013).
- [42] M. Li, C. Chen, and W. Liu, "Identification based on MATLAB," in *Proc. Int. Workshop Inf. Secur. Appl. (IWISA)*, 2009, pp. 523–525.



**CHIH-HO TAI** was born in Taichung, Taiwan. He received the master's degree in industrial engineering from National Taiwan University, where he is currently pursuing the Ph.D. degree with the Department of Mechanical Engineering. He has a mechanical patent for a thermal acupuncture machine. His research interests include laser processing and precision machining.



**YING-TE TSAI** received the master's degree from the Department of Mechanical Engineering, National Taiwan University. He is currently a Product Design Engineer with Apple Inc., where he works on component design, manufacturing design, and failure analysis for Apple products.



**KUAN-MING LI** received the Ph.D. degree from the Department of Mechanical Engineering, Georgia Institute of Technology, USA. He is currently an Associate Professor with the Department of Mechanical Engineering, National Taiwan University, Taipei, Taiwan. His current research interests include machining process modeling and monitoring, incremental forming, and the applications of artificial intelligence in manufacturing processes.